International Journal on Magnetic Particle Imaging
Vol 10, No 1, Suppl 1, Article ID 2403039, 5 Pages

Infinite Science Publishing

Proceedings Article

Design of a magnetic particle imaging integrated with magnetic hyperthermia by aiming at pediatric cancer treatment

Thanh-Luu Cao[a,†] · Seungjun Oh[a,†] · Tuan-Anh Le[b] · Minh Phu Bui[a] · Muhammad Umar Tahir[a] · Hafiz Ashfaq Ahmad[a] · Jungwon Yoon[a,*]

[a]School of Integrated Technology, Gwangju Institute of Science and Technology, Gwangju 61005, Republic of Korea
[b]Department of Physiology and Biomedical Engineering, Mayo Clinic, Scottsdale, Arizona 85259, USA
[†]Equally contributed to this paper
[*]Corresponding author, email: jyoon@gist.ac.kr

Abstract

Magnetic Particle Imaging (MPI) is an emerging non-invasive medical imaging method capable of determining the concentration and spatial distribution of superparamagnetic iron oxide (SPIO) nanoparticles. Ongoing research is exploring technology to estimate the temperature of particles based on MPI signals. In magnetic hyperthermia treatment, volumetric temperature measurement is crucial for ensuring the safety of healthy tissues. While the efficacy of magnetic hyperthermia and simulation-based methods for estimating temperature and damage is now recognized, no prior studies have reported a human-sized MPI system that integrates hyperthermia and MPI. Such integration could potentially allow for non-invasive treatments. In this paper, we present the design and manufacture of a theranostic platform with the potential for MPI, magnetic hyperthermia and thermometry. The development of such technology could greatly extend the application of MPI in planning magnetic hyperthermia treatments.

I. Introduction

The magnetic particle imaging (MPI) device is a relatively new imaging modality that can determine the concentration and spatial distribution of superparamagnetic iron oxide (SPIO) nanoparticles using their nonlinear magnetization response to an alternating magnetic field [1]. It is radiation-free and capable of high-resolution, high-sensitivity, and real-time imaging, making it suitable for various medical applications such as vascular and perfusion imaging, oncology imaging, cell tracking, inflammation imaging, trauma imaging, navigation for magnetic drug delivery, and magnetic hyperthermia [2, 3]. In magnetic hyperthermia, heat generated due to the magnetization reversal process in magnetic nanoparticles (MNPs) during the application of a radiofrequency magnetic field is employed to treat cancer [4]. Although MagForce has reported several clinical trials of magnetic hyperthermia, it has not yet been translated into clinical routine worldwide. There are various challenges for this translation; particularly, the MNPs spatial distribution in tissues, difficulty in delivering the applied magnetic field in a targeted manner, and the lack of a real-time, noninvasive, and volumetric temperature measurement.

It has been shown that MPI can stand out as a promising candidate to address these aforementioned challenges. It can accurately determine the particles distri-

bution and concentration in real-time. If combined with a magnetic hyperthermia device, its magnetic field gradient can provide arbitrary localized heating [5, 6]. Finally, it has been proven that the changes in the higher harmonics of the acquired signal with temperature can be used as a tool for thermometry [7, 8, 9].

Localized (focused hyperthermia using MPI) can be a promising approach for minimizing damage to healthy tissues. However, except for special cases such as using superconductors [10], when scaling up the MPI scanner for human sizes, its magnetic field gradient strength reduces substantially. This is while in focused hyperthermia, the magnetic field gradient plays a crucial role [6, 11]. An alternative approach can be the development of human-sized MPI scanners that can accommodate a magnetic hyperthermia coil in its bore. In this approach, the integrated device can be used for determining the MNPs distribution, applying radiofrequency magnetic field for hyperthermia, and performing volumetric MPI thermometry by inspecting the changes in higher harmonics with temperature.

Children with cancer, despite improved survival from combined therapies like chemotherapy, surgery, and radiation, still face risks due to intensified treatments, especially with metastatic sarcoma and recurrent solid tumors. Innovating new therapies that minimize immediate and long-term side effects is crucial. Recent advancements in non-invasive heat-based therapies show promise for safe, targeted treatments, potentially transforming pediatric cancer care [12]. Therefore, in this paper, we designed and developed a MPI scanner combined with a hyperthermia device with the potential for pediatric cancer treatment.

The device has a hexahedral workspace (bore size) measuring 232×332×550 mm^3. For scanning in the x-axis, it uses a single-axis motor for mechanical movement (175mm to the left and right side). This, along with electric steering of its field-free-point (FFP) in z- axis and y-axis allows covering most of a child's body up to 14 years old [13]. The body sizes may differ case to case, but the average sizes reported in [14] can be accommodated in the device comfortably.

The amplitude modulation (AM) method was utilized for image reconstruction [15]. In AM MPI, a low frequency and high amplitude magnetic field is used to steer the FFP, while a high frequency and low amplitude one excites the magnetic nanoparticles (MNPs) [15, 16]. Two main advantages of AM MPI are mitigating the risk of peripheral nerve stimulation (PNS) and the possibility of using a wide bandwidth receiver coil. The current device, by integrating hyperthermia and MPI, has the potential to serve as a theranostic platform for magnetic hyperthermia treatment.

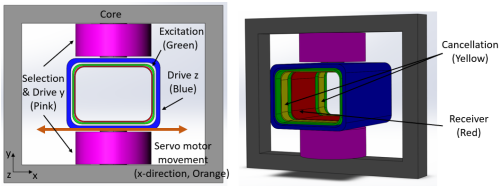

Figure 1: Coil topologies and system configuration of the proposed MPI system

II. Material and Methods

II.I. System Configuration

MPI System: The system configuration for the proposed MPI system is shown in Fig. 1. The system includes a soft core to improve the selection field and a single-axis servo motor for moving the workspace in the x-axis. It moves with 5mm step and low speed of 5mm/s. Here, the fixed part includes the core and the selection & drive y, while the movable parts (inner coils) are excitation, drive z, receiver, and cancellation coils.

To reduce system size, the selection coil and drive y coil are integrated into one pair of coils in a Maxwell configuration to generate the FFP at the center. The role of the coil can be determined depending on the frequency and amplitude of the applied current. The single-axis servomotor located at the bottom of the inner coil can move the inner coil in the x-axis direction. This serves as a replacement for the drive x coil. The movement is performed to select each scanning plane for 2D image. Then a 3D image is composed of multiple 2D images.

The inner coils are organized along the z-axis. The drive z coil for moving the FFP in the z direction is also located along the z-axis. In combination with the drive coil y, the FFP can be steered in the yz-plane to create a two-dimensional FOV. The yz-plane thus created is moved in the x-direction in 5 mm steps by the servo motor, ultimately creating a three-dimensional FOV. The receiver coil is located in the center of the inner coils, and the cancellation coil, in two parts, is located close to the receive coil. A water-cooling system is used for the selection & drive y coil and operates in connection with an external cooler.

Magnetic hyperthermia system: The magnetic hyperthermia system was designed to be accommodated within the workspace of the MPI system. For this purpose, a pancake coil configuration was chosen and 16 kW power system was selected while considering magnetic field amplitude. Although the magnetic field amplitude reduces by distance from the surface of the coil, the strong magnetic field produced by the device at surface (H=50 kA/m and f=120 kHz) can guarantee usable fields for hyperthermia at depths of up to 5 cm (H=15 kA/m). After designing the hyperthermia system, it was further optimized and manufactured by Ultraflex Corp.

10.18416/ijmpi.2024.2403039

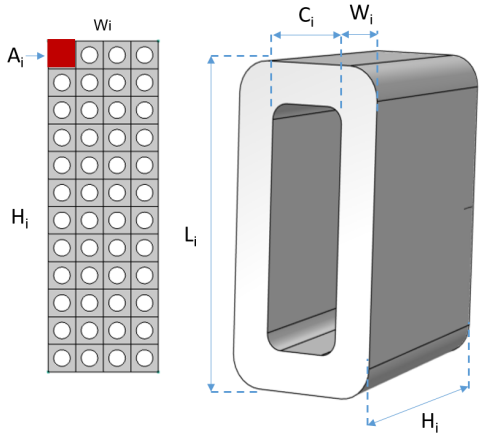

Figure 2: The control variables for the proposed system design.

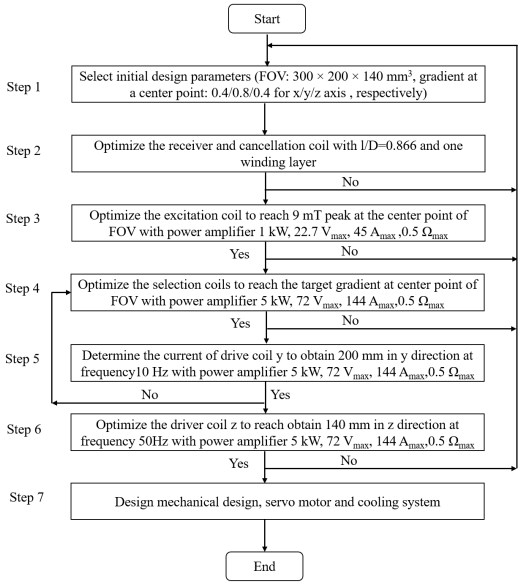

Figure 3: The optimization process for the proposed system design.

II.II. The Method

To optimize the system design, COMSOL Multiphysics software (COMSOL AB, Stockholm, Sweden) was utilized with the Nelder-Mead method to find the optimized design. Our target was to achieve a gradient of 0.4/0.8/0.4 (T/m) for the x/y/z axis in a FOV of 300 × 200 × 140 mm^3. The control variables, such as the width W_i, height H_i, length L_i, core C_i and current I_i of each coil were shown in Fig. 2. With our existing power amplifiers (5kW for AE Techron 7794 and 1kW for AE Techron 7224), we can optimize the coil dimensions and the number of turns which are calculated as N_i=H_i*W_i/A_i where Ai is the cross-sectional area of the winding wire. A hollow squared conductor was utilized for the selection and drive coils while Litz wire was used for the excitation and receiver coils to prevent the skin effect at high frequencies. The optimization process is presented in Fig. 3. To optimize the coils, the objective function was defined as $F = (p/p_{target} - 1)^2$ where p and p_{target} indicate the measured and desired targets for each coil, respectively. LabVIEW (National Instruments, Texas, USA) and MATLAB (MathWorks, Natick, MA, USA) codes were written for temperature estimation based on higher harmonics and image reconstruction based on amplitude modulation [15].

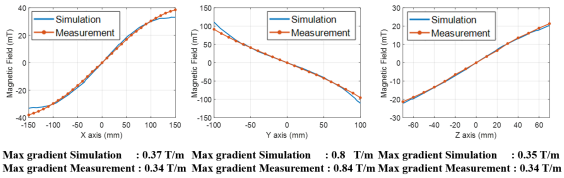

Figure 4: Simulation and experimental results of magnetic field gradient for (a) x-axis, (b) y-axis, and (c) z-axis.

III. Results and discussion

Fig. 4 shows the simulated and measured magnetic field gradient of the MPI scanner. As can be seen, magnetic field gradients of 0.37 T/m, 0.8 T/m, and 0.35 T/m can be achieved for the x/y/z axis, respectively. These were achieved by applying a current of 50 A to the selection coil. For standard particle of 30nm, we can achieve 3∼4 mm resolution [17], meaning we can estimate the temperature of particles within an area of 256 mm^3. With these gradients, we expect to acquire 3D MPI images for determining MNPs concentration and distribution and obtain temperature maps at different instances of magnetic hyperthermia procedure targeting cancers. It should, however, be mentioned that for acquiring these images, the magnetic hyperthermia device needs to be turned off to prevent interference from its magnetic field. Therefore, the system must be optimized to perform real-time thermometry to obtain meaningful information about the temperature during hyperthermia.

A photograph of the proposed MPI system is shown in Fig. 5. For the stability and convenience of the experiment, an additional movable stand was manufactured, and the overall system size, including the stand, is 1545×1324×942 mm^3. The target specifications of the system parameters are provided in Table 1. Due to the symmetry of the inner coils the pancake coil of the magnetic hyperthermia device can be located on either side of the MPI system. The coil length is designed such that it can be in the center of the receive coil.

10.18416/ijmpi.2024.2403039

Table 1: Targeted characteristics of the system parameters

Parts	Selection/driver y coil	Driver coil z	Excitation coil	Receiver/Cancellation coil
Max current [A]	70 (50/20)	54.82	35.36	-
Max current density [A/mm^2]	3.14	2.15	2.67	-
Conductor type	Squared shape	Squared shape	Litz wire	Litz wire
Coil size (horizontal) [mm]	6	6		
Coil size (vertical) [mm]	6	6	1500/AWG	420/AWG
Hollow diameter [mm]	3.5	3.5	38	46
Number of turns per a coil	416	249	91	25
Coil copper area [mm^2]	25.52	25.52	11.95	0.5235
Coil cross area [mm^2]	43.56	43.56	11.95	0.5235
Turn insulation [mm]	0.3	0.3	-	-
Resistance per a coil [Ω]	0.5	0.22	0.145	-
Voltage [V]	35.2	12.03	5.12	-
Power [kW]	2470	660	181	-
Maximum gradient (x/y/z) [T/m]	0.37/0.8/0.35			
FOV (x/y/z) [mm]	300×200×140			

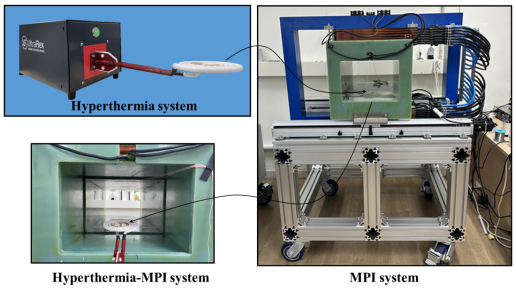

Figure 5: Manufactured theranostic platform

IV. Conclusions

The proposed system has the potential to address the scalability issues present in existing MPI systems. It can act as an independent theranostic platform for magnetic hyperthermia in pediatric cancers. Exploiting the full potential of such a system not only facilitates hyperthermia for patients through non-invasive thermometry, but also prevents damage to healthy tissue through temperature monitoring. Verification of the 3D MPI imaging test and temperature measurement system will be conducted and reported in future works.

Author's statement

Research funding: This work was supported by the Korea Medical Device Development under Grant 202012E12.
Conflict of interest: Authors state no conflict of interest.

References

[1] B. Gleich and J. Weizenecker, "Tomographic imaging using the nonlinear response of magnetic particles", Nature, vol. 435, no. 7046, pp. 1214-7, 2005, doi: 10.1038/nature03808.

[2] T. Knopp, N. Gdaniec, and M. Möddel, "Magnetic particle imaging: from proof of principle to preclinical applications," Physics in Medicine & Biology, vol. 62, no. 14, p. R124, 2017, doi: 10.1088/1361-6560/aa6c99.

[3] Chandrasekharan, P., Tay, Z. W., Hensley, D., Zhou, X. Y., Fung, B. K., Colson, C., ... & Conolly, S., "Using magnetic particle imaging systems to localize and guide magnetic hyperthermia treatment: tracers, hardware, and future medical applications," Theranostics, Review vol. 10, no. 7, pp. 2965-2981, 2020, doi: 10.7150/thno.40858.

[4] D. Ortega and Q. Pankhurst, "Magnetic Hyperthermia," vol. 1, pp. 60-88, 2013.

[5] Tay, Z. W., Chandrasekharan, P., Chiu-Lam, A., Hensley, D. W., Dhavalikar, R., Zhou, X. Y., ... & Conolly, S. M. "Magnetic particle imaging-guided heating in vivo using gradient fields for arbitrary localization of magnetic hyperthermia therapy." ACS nano, 12.4, 2018, 3699-3713, doi: 10.1021/acsnano.8b00893

[6] T.-A. Le, Y. Hadadian, and J. Yoon, "A prediction model for magnetic particle imaging–based magnetic hyperthermia applied to a brain tumor model," Computer Methods and Programs in Biomedicine, vol. 235, p. 107546, 2023, doi: doi: 10.1016/j.cmpb.2023.107546.

[7] RAUWERDINK, Adam M.; HANSEN, Eric W.; WEAVER, John B. Nanoparticle temperature estimation in combined ac and dc magnetic fields. Physics in Medicine & Biology, 54.19: L51, 2009, doi: 10.1088/0031-9155/54/19/l01

[8] A. M. Rauwerdink, E. W. Hansen, and J. B. Weaver, "Nanoparticle temperature estimation in combined ac and dc magnetic fields,", Phys Med Biol, vol. 54, no. 19, pp. L51-5, 2009, doi: 10.1088/0031-9155/54/19/l01.

[9] Salamon, J., Dieckhoff, J., Kaul, M. G., Jung, C., Adam, G., Möddel, M., ... & Ittrich, H. Visualization of spatial and temporal temperature distributions with magnetic particle imaging for liver tumor ablation therapy. Scientific Reports, 10.1: 7480., 2020, doi: 10.1038/s41598-020-64280-1

[10] Le, T. A., Bui, M. P., Gadelmowla, K. M., Oh, S., & Yoon, J. , "First Human-scale Magnetic Particle Imaging System with Superconductor.," International Journal on Magnetic Particle Imaging IJMPI 9.1 Suppl 1 2023, doi: 10.18416/IJMPI.2023.2303032

[11] S. Healy, A. F. Bakuzis, P. W. Goodwill, A. Attaluri, J. W. M. Bulte, and R. Ivkov, "Clinical magnetic hyperthermia requires integrated magnetic particle imaging," (in eng), Wiley Interdiscip Rev Nanomed Nanobiotechnol, vol. 14, no. 3, p. e1779, 2022, doi: 10.1002/wnan.1779.

[12] C. Tydings, K. V. Sharma, A. Kim, and P. S. Yarmolenko, "Emerging hyperthermia applications for pediatric oncology," Advanced Drug Delivery Reviews, vol. 163-164, pp. 157-167, 2020, doi: https://doi.org/10.1016/j.addr.2020.10.016.

[13] K. U. I. Feng, L. I. Chen, S.-M. Han, and G.-J. Zhu, "Ratio of waist circumference to chest circumference is inversely associated with lung function in Chinese children and adolescents," Respirology, vol. 17, no. 7, pp. 1114-1118, 2012, doi: 10.1111/j.1440-1843.2012.02219.x.

[14] PIERCE, Jeanne Walsh; WARDLE, Jane. Self-esteem, parental appraisal and body size in children. Journal of Child Psychology and Psychiatry, 34.7: 1125-1136., 1993, doi: 10.1111/j.14697610.1993.tb01778.x

[15] T. A. Le, M. P. Bui, and J. Yoon, "Development of Small Rabbit-scale Three-dimensional Magnetic Particle Imaging System with Amplitude Modulation Based Reconstruction," IEEE Transactions on Industrial Electronics, pp. 1-1, 2022, doi: 10.1109/TIE.2022.3169715.

[16] X. Zhang, T. A. Le, A. K. Hoshiar, and J. Yoon, "A Soft Magnetic Core can Enhance Navigation Performance of Magnetic Nanoparticles in Targeted Drug Delivery," *IEEE/ASME Transactions on Mechatronics*, vol. 23, no. 4, pp. 1573-1584, 2018, doi: 10.1109/TMECH.2018.2843820.

[17] GOODWILL, Patrick W.; CONOLLY, Steven M. The X-space formulation of the magnetic particle imaging process: 1-D signal, resolution, bandwidth, SNR, SAR, and magnetostimulation. *IEEE transactions on medical imaging*, 29.11: 1851-1859, 2010, doi: 10.1109/TMI.2010.2052284.

